CrossMark

ORIGINAL ARTICLE

Assessment of the state of soils, shallow sediments and groundwater salinity in Abi, Cross River State, Nigeria

Anthony E. Akpan · Ebong D. Ebong · Stephen E. Ekwok

Abstract Abi area in Nigeria borders the salinity enriched Lower Benue Trough (LBT) and plans are currently underway to extend large-scale irrigation facilities under construction in the LBT to Abi area. In order to generate baseline soil and water salinity information about Abi area under non-irrigation condition, integrated information from constrained analyses of vertical electrical sounding data, two-dimensional electrical resistivity tomographies and laboratory analyses of soil and water samples were used to assess and map the spatial salinity distribution. Existence of widespread heterogeneities in the distribution of soil and water salinity between the shaly and sandy materials that dominate the shallow geology of the area was observed. Minimum values of water electrical conductivity (WEC) and total dissolved solids (TDS) were observed to be 19.2 µS/cm and 13 mg/L, respectively, in the sandstone-dominated areas. Maximum values of WEC and TDS were observed to be 931.0 µS/cm and 624 mg/L, respectively, within the shale-dominated areas. Soil electrical conductivity was observed to vary from 5.0 µS/cm in the sandstone areas to 14.0 µS/cm in the shale-dominated areas. Minimum and maximum soil pH observations were 4.53 in the shale-dominated area and 6.55 in the sandstone-dominated area, respectively. These results show that the water and soil resources in the area vary from fresh to slightly saline and non-saline to high salinity levels, respectively. Consequently, both resources are still good for agricultural purposes.

Introduction

Coastal communities in Nigeria occupy a strategic position in the economic development of the country and have consequently witnessed unprecedented growth in population because of increased urbanization, agricultural and industrial activities. These developments have attracted diverse interest groups such as job seekers, businessmen and industrialists to the coastal areas. In many of such coastal communities, the rapid surge in human population took the local authorities unawares thereby overstretching some of the available natural resources including groundwater and soils. Excessive pumping of groundwater resources in coastal areas can threaten the availability of potable water for domestic and other needs because it can induce saline water to flow into the fresh water aquifers and consequently contaminate it (Edet et al. 2011; Adepelumi et al. 2008). Other urban related anthropogenic activities that can also induce saline water flow into coastal aquifers include excessive paving (Chang et al. 2011). In many of the affected coastal communities, soil productivity is seriously impaired leading to food shortages.

In responding to the problems of food shortages, government at all levels and other development partners have been embarking on sensitization campaigns and necessary reforms directed at encouraging people to embrace modern agricultural practices. In order to ensure sustainable food production, farmers have embraced irrigation farming and other yield enhancement practices such as the excessive application of inorganic fertilizers, herbicides and pesticides that can also threaten the potability of groundwater

A. E. Akpan (✉) · E. D. Ebong · S. E. Ekwok
Applied Geophysics Programme, University of Calabar,
PMB 1115, Calabar, Cross River State, Nigeria
e-mail: anthonyakpan@yahoo.com

and soil productivity levels (Benkabbour et al. 2004; Young et al. 2007; Sikandar et al. 2010; Poulsen et al. 2010). Water for irrigation is usually sourced from dams and where available, the surface water resources can also be exploited for this purpose. Such farming practices are known to degrade groundwater quality through increase in salinity, loss of soil nutrients and biodiversity (Poulsen et al. 2010; Chang et al. 2011; Nwankwoala 2011).

Recently, there has been intense research on groundwater salinization pattern and its effects on soil and crop yield in many parts of the world (Benkabbour et al. 2004; Vandenbohede et al. 2009; Sikandar et al. 2010; Zarroca et al. 2011; Chang et al. 2011). Most of the natural resources including groundwater and soil in the Benue Trough, Central Nigeria are characterised by elevated primary salinity. Studies conducted so far have been primarily directed at characterising these resources and inferring the source of the enhanced salinities (Egboka and Uma 1986; Uma et al. 1990; Tijani et al. 1996; Tijani 2004), isotopic composition (Tijani 2008) and water quality (Edet et al. 2011). Central Nigeria is the hub of agricultural practice and presently, many dams and irrigation facilities are currently being constructed by the Government for use by the farmers although studies by Edet et al. (2011) have shown that the groundwater resource in the Benue Basin is not suitable for agricultural purposes.

Although Abi is located at the fringe between the saline water enriched Lower Benue Trough and the fractured sandstone aquifers of the Asu River Group (Akpan et al. 2013; Ebong et al. 2014), no reports of salinity enrichment problems exist. The dams and other irrigation facilities under construction in the adjoining states may supply water to the farmers in Abi area and this therefore calls for close monitoring of salinity levels in both soil and water resources in the area. Time lapse salinity monitoring programmes are usually based on a good knowledge of aquifer type, characteristics, spread, groundwater quality, salinity and evolution (Zarroca et al. 2011). Conventional techniques of monitoring soil and groundwater salinity conditions and their dynamic fluctuations are grouped into the direct and indirect investigative methods. The direct methods consist of the traditional sampling techniques such as the use of geochemical tracers, soil and water sampling (Swarzenskis et al. 2007; Young et al. 2007; Moore and de Oliveira 2008) and numerical simulation studies (Mao et al. 2005; Michael et al. 2005; Vandenbohede et al. 2008). For large-scale surveys, the direct sampling technique is usually expensive, time consuming, invasive and consequently environmentally unfriendly. The indirect approach involves inferring the spatial distribution of soil and groundwater characteristics from measured geophysical data. The geophysical approach is economical, fast, non-invasive and environmentally friendly but results are sometimes fraught with errors arising from ambiguities inherent in the transformation of the geophysical data to their equivalent geological models (Ebong et al. 2014; Toushmalani 2010). These ambiguities are usually resolved by correlating geophysical data with either geological data acquired at a location nearest to the geophysical station or other geophysical techniques or both (Cardarelli et al. 2010).

The aim of this study is to use information generated from constrained inversion of electrical resistivity data and direct sampling of soil and groundwater to assess the spatial distribution of salinity in Abi, Nigeria.

Site description

Location

Abi area is located between latitudes 5°45′N and 6°05′N of the equator and longitudes 7°55′E and 8°12′E of the Greenwich Meridian in Cross River State, Nigeria (Fig. 1a). Abi is bounded in the north and west by Ikwo and Afikpo areas of Ebonyi State, Nigeria. The eastern boundary of Abi is shared with Yakurr and Obubra areas and to the south by Biase area all in Cross River State, Nigeria.

The area is characterised by a humid tropical climatic condition that is made up of two seasons: the wet (March–October) and dry (November–April). Rainy (wet) season begins in March when the Atlantic Ocean borne warm and moisture laden tropical maritime air mass blows northward across the area and ends in October. The dry season, which occurs in the rest of the months, is a period when the tropical continental air mass that originates from the Sahara blows across the area. In the dry season, most of the surface water and even shallow groundwater resources do dry up creating severe water scarcity.

Geology and stratigraphy

Abi is located in the Ikom Mamfe Embayment (IME) in Central Cross River State. The IME is a NW–SE splay segment of the NE–SW trending Benue Trough. The basin extends laterally into parts of Western Cameroon where it covers an estimated area of about 2,016 km² (Eseme et al. 2002). The Abakaliki Anticlinorium, Oban Massif, Obudu Plateau and the Cameroon Volcanic Line, respectively (Fig. 1b, c), bound the IME in the western, southeastern, eastern, and northeastern.

Sedimentation in the IME commenced with the deposition of the marine Albian Asu River Group (ARG) (Fig. 1a) on the Precambrian Basement. The basement is intruded by pegmatite in some locations (Eseme et al.
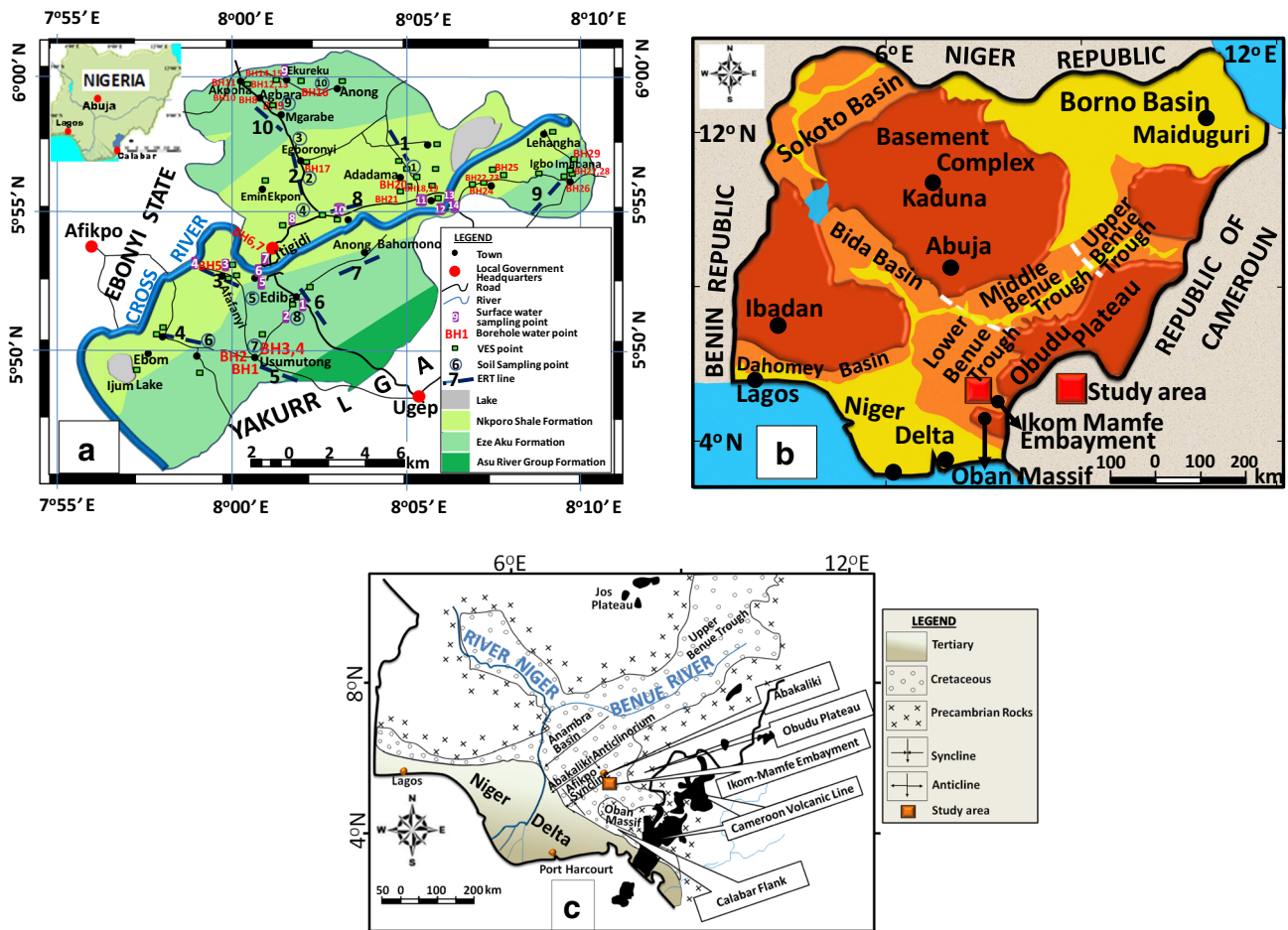
Fig. 1 **a** Geologic map of Abi area showing VES, soil and water sampling points. *Insert* Map of Nigeria showing the position of Cross River State (*blue*), **b** Generalised geologic map of Nigeria showing the location of the study area and **c** geologic map of the Benue Trough showing locations of Abakaliki Anticlinorium, Afikpo Syncline, Ikom Mamfe Embayment, Oban Massif and the Cameroon Volcanic Line

2002). The dominant regional strike direction of geologic structures is N–S although some occasional NE–SW swings have also been reported (Ekwueme et al. 1995). Non-marine to marginal marine sediments dominate the ARG. Intercalating ammonite bearing limestones and sandstones (Odigi and Amajor 2008) usually truncate the vertical continuity of the thick shales.

Late Albian-Cenomanian impervious calcareous and non-calcareous black shales, siltstones and sandstones of the Eze-Aku Formation (EAF) overlie the ARG (Fig. 1a). These Cretaceous sediments are deformed and occasionally intruded by dense, fine-grained and sometimes dark coloured Tertiary rocks such as basalts and dolerites. The Cameroon Volcanic Province borne and other low-grade metamorphic activities occur in the area and have been identified as the major cause of deformation of the sediments and basement materials (Morreau et al. 1987). The sediments acquired secondary porosities essential for fluid transmission in the process of being deformed. Other activities of tectonic origin that contributes to stratal

dislocation, fault and fracture reactivation include the episodic compressive earth movements in the post-Santonian (Odigi and Amajor 2009). These deformations produce multiple folds and fractures that are oriented parallel to the fold axis. The Abakaliki Anticlinorium and the Afikpo Syncline (Fig. 1c) are two major products of these tectonic disturbances (Onwualu et al. 2012). Thus, the underlying Cretaceous sediments are highly baked, domed and deformed in many locations in the area (Benkhelil 1982).

The Nkporo Shales Formation (Fig. 1a) overlies the EAF. It consists of thick-bedded shales that are reflective of funnel-shaped shallow marine setting that eventually graded into low-energy marshes.

Hydrogeology

Abi is drained by the NE–SW flowing Cross River, streams, ponds and lakes while seepages from the hills and ridges fill the low-lying areas. The low-lying areas are

always poorly drained due to the blocking of the water flow paths by the hills and ridges. The resulting situation causes the entire low-lying areas to always be wet and swampy particularly in the rainy season. In the dry season, when the primary source of recharge (rainfall) ceases, the surging heat of the tropical sun will cause the water in the low-lying areas to dry up. The hitherto wet clays and other argillaceous materials will dry up and pressure cracks will be formed on them.

Studies show that majority of water sources in the Benue Trough and adjoining areas are saline and has been detected based on laboratory analyses of water samples from disseminated salt ponds, hand dug wells, springs and boreholes (Edet et al. 2011; Tijani 2004, 2008). Early researchers attempted to associate groundwater salinization in the Benue Trough with some geologic structures (e.g., fractures) and mineralised veins (e.g., galena, sphalerite, barite, fluorite, pyrite and silver) (Tijani 2004, 2008; Tijani and Loehnert 2004), although the areal extent of saline water mineralization is more extensive than the zones where the occurrence of these tectonic elements and mineralized veins have been mapped.

Abi is located within the middle course of the Cross River where the river exhibits a sluggish and meandering flow pattern with high deposits of sand at the beaches. The volume of water and the amount of sediments that the Cross River transports across the area are season dependent. At the peak of the dry season, the volume of water in the river drops considerably and water flows are limited to narrow channels in the river bed. During the wet season, there is a rapid rise in water levels in the Cross River and its tributaries.

Materials and methods

Electrical resistivity data acquisition

Electrical resistivity techniques [electrical resistivity tomography (ERT) and the vertical electrical sounding (VES)] are popular members of the conventional geophysical investigating tools. They are used in mapping shallow subsurface electrostratigraphy based on observed contrast in resistivity between the different lithologic units in a geologic formation. The electrical resistivity method has well-established theory, documented in many geophysics textbooks and other relevant literatures like Keller and Frischknecht (1966), Telford et al. (1990) and so on. Several researchers have successfully applied the electrical resistivity method in solving a wide range of hydrological and hydrogeophysical problems including mapping of saturated aquifer horizons from the adjoining formations, groundwater potential investigations, aquifer characterisation, assessment of infiltration rate of the vadose zone and groundwater contamination studies (Inoubli et al. 2006; Samsudin et al. 2007; Ogilvy et al. 2008; Gemail et al. 2011; Minsley et al. 2011; Akpan et al. 2009, 2013; Ebong et al. 2014).

The bulk electrical resistivity is an intrinsic property of geologic formations and relates to rock properties like porosity, extent of saturation, nature of the saturating fluid and diagenetic cementation factors (Archie 1942). Archie's law establishes a petrophysical relationship that relates measured bulk resistivity (ρ) of a completely saturated clean sand formation to its porosity (ϕ) and pore fluid resistivity (ρ_w) as,

$$\rho = \alpha \cdot \rho_w \cdot \phi^{-m} \tag{1}$$

where α and m are formation dependent constants. The coefficient α (sometimes called the tortuosity index) expresses the extent of connectivity of the pores spaces in a formation, while m is associated with the level of cementation of the geologic materials (Metwaly et al. 2006). Archie's law is valid in geologic formations where infill pore fluid is the only medium of electrical conduction. But in geologic formations such as clays, shales and some metallic ores where the rock grains can conduct electricity, Archie's law will breakdown (Minsley et al. 2011). Several models of electrical current conduction in the event of Archie's law breakdown have been developed in such environments but majority of them fall into either shale-fraction or cation-exchange model derived empirically using the concept of parallel conduction (Sen et al. 1998).

Sediments of the ARG underlie most of the communities in Abi where records of tecto-thermal disturbances exist. However, the influence of clay and clay-derived sediments in the area was carefully considered as these sediments can significantly degrade results computed from Archie's law. The use of Hanai–Bruggeman effective medium theory (EMT), which recognises the contributions of rock grain conductivity (σ_r) in the computation of bulk conductivity (Bussain 1983) (Eq. 2), and has been successfully used in estimating electrical resistivity in such environments (Acworth and Jorstad 2006) was considered.

$$\sigma_b = \sigma_w \cdot \alpha \cdot \varphi^m \left(\frac{\left(1 - \frac{\sigma_r}{\sigma_w}\right)}{\left(1 - \frac{\sigma_r}{\sigma_b}\right)} \right)^m \tag{2}$$

But in our study area, continuous human activities like farming, movement of heavy duty farming equipment and road construction that have been going on in the area, have caused serious compaction of the superficial sediments. Such compaction processes can lead to significant reduction in porosity (Schutjens et al. 2004; Beriss et al. 2012; Wang et al. 2012). Consequently, we assumed that contributions from grain surface conductivity was negligibly small since our depth of interest is shallow and

therefore was ignored. The implication of this assumption is that the σ_r term in Eq. 2 can be ignored thereby making Eq. 2 to revert to Eq. 1.

Inspired by the successful application of electrical resistivity method, we adopted an integrated approach involving lithologic information from existing borehole data, geologic information from directly measured soil and groundwater parameters such as pH, total dissolved solids (TDS) and the electrical conductivity (EC) of the samples and electrical resistivity information to assess the spatial distribution of soil and groundwater salinity in Abi, Nigeria.

Fifty-five randomly sited but fairly distributed VESs were performed in the area in two phases between January 2011 and March 2012. The IGIS (India) resistivity meter and stainless steel electrodes were used for VES data acquisition while the 2-D ERT data were acquired using ABEM terrameter SAS 1000 and the ES 10-64 switching unit. Minimum current electrode spacing (AB) used in VES data acquisition was 1 m while maximum current electrode separations were constrained by settlement pattern, topography and other unfavourable field conditions to vary between 500 and 600 m. Corresponding receiving (potential) electrode separation (MN) varied from 0.5 m at AB = 1 to 40 m at AB = 600 m. Eight ERT profiles with length 100 m each were occupied in the first phase while in the second phase, ERT data were acquired along two profiles with similar profile length. Some of the ERT profiles cross the VES points so that results can be correlated. All the ERT lines were located on a relatively plane ground where elevations were less than 40 cm in order to reduce the influence of topography on the data. Minimum electrode spacing (a) was 3 m while maximum electrode spacing was 33 m (corresponding to 11a).

Although the Abi area is not expected to be electrically noisy except at few locations where power transmission and distribution facilities pass directly overhead, the Wenner electrode array, which can generate data with good vertical resolution and high signal to noise ratio was used in acquiring the ERT data (Loke et al. 2003; Gómez-Ortiz et al. 2007). The reciprocal error technique in which 5 % was set as the maximum acceptable value was also used for in situ assessment of the ERT data quality. The reciprocal error was computed using Eq. 3 and it was performed by interchanging the current and potential electrode pairs.

$$e = 100 \frac{|\rho_n - \rho_r|}{\rho_n + \rho_r} \tag{3}$$

In many stations, the reciprocal error was less than 5 % but where occasional high error swings were observed, measurements were repeated. Prior to the main data acquisition exercise, all the electrodes were carefully checked for contact resistance problems and it was observed that over 95 % of all the electrodes were in good electrical contact with the ground having contact resistances that vary between 200 and 300 Ωm (Wilkinson et al. 2010). Measures that were taken to minimise contact resistance problems include wetting of the electrode positions with water and where necessary, with salt solutions and driving the electrodes deeper into the argillaceous (or arenaceous) sediments (Arango-Galván et al. 2011).

Soil and groundwater sampling

Soil and water (surface and groundwater) samples were collected in selected locations within the study area at the same period that the geophysical investigations were being conducted. These samplings were necessary in calibrating the electrical resistivity data of the shallow subsurface and validating the geophysically generated results. A total of 43 water samples consisting of 29 groundwater and 14 surface water samples were collected. In situ measurements of water electrical conductivity (WEC), pH and temperature of all the water samples were made at all the sampling points using a Combo EC and pH meter (Hanna HI98130) from Hanna Instruments, USA. An estimate of the TDS in the water samples was made by multiplying the observed WEC values by a factor of 0.67 (Weyl 1964; Yihdego and Webb 2012). Results obtained are shown in Table 1.

Undisturbed representative soil samples were collected from 10 locations at 0.5 m depth using soil sampling ring kits from Eijkelkamp Equipment, Netherlands. The samples were analysed in the laboratory for the purpose of determining their soil electrical conductivity (SEC) and pH. The samples were crushed, air-dried and all particles larger than 2 mm were sieved out using a 2 mm size sieve. A suspension consisting of soil samples and deionised water in the ratio of 1:5 was prepared. The suspension was shaken for over 90 min to enable all soluble salts to dissolve properly. The SEC and pH were measured using a pre-calibrated conductivity and pH meter. Results of laboratory analyses of the soil samples are shown in Table 2. The SEC values determined from the direct method were correlated with SEC values estimated from the indirect electrical resistivity method (i.e., VES) (Table 2). Using a GPS map 76 model of a Garmin global position system, geographic coordinates of each sounding point, ERT profiles, soil and water sampling points were measured for proper location of the points on the map as well as graphical representation of the data.

Data analysis

The measured field resistances were converted to apparent resistivities by multiplying the measured apparent resistances with their corresponding geometrical factor for both

Table 1 Results of groundwater conductivity, temperature, estimated TDS and pH

Location	Water sample type	Coordinates (°)		Elevation (m)	Temperature (°C)	TDS (mg/l)	pH	Measured conductivity corrected to 25 °C (μS/cm)	Water class for irrigation purposes*
		Longitude (E)	Latitude (N)						
Usumutong	BH1	8.019	5.830	46	27	338	4.5	504.96	Good
	BH2	8.019	5.828	47	27	313	3.8	467.52	Good
	BH3	8.016	5.831	50	27	320	4.8	478.08	Good
	BH4	8.006	5.843	101	28	88	3.2	130.66	Excellent
Afafanyi	BH5	7.991	5.888	38	27	14	1.4	21.12	Excellent
	BH6	8.020	5.887	48	29	69	3.6	103.04	Excellent
Itigidi	BH7	8.018	5.886	32	28	20	1.9	30.08	Excellent
Agbara	BH8	8.021	5.984	44	28	407	4.3	608.18	Good
Akpoha	BH9	8.021	5.984	63	28	447	5.2	667.40	Good
	BH10	8.020	5.985	49	28	317	3.6	472.82	Good
Akarafor	BH11	8.017	5.988	43	28	491	3.5	733.20	Good
	BH12	8.018	5.988	50	28	110	1.2	164.50	Excellent
	BH13	8.013	5.992	53	28	136	3.4	203.04	Excellent
	BH14	8.014	5.994	38	28	142	2.1	212.44	Excellent
Ekurekube	BH15	8.016	5.993	46	28	115	1.5	171.08	Excellent
	BH16	8.016	5.987	66	28	60	2.6	89.30	Excellent
Egboronyi	BH17	8.037	5.947	48	28	266	3.6	396.68	Good
Atani-Adadama	BH18	8.088	5.928	37	26	488	4.3	728.14	Good
	BH19	8.089	5.927	38	31	435	5.1	649.44	Good
Ekpon-Adadama	BH20	8.081	5.930	30	26	462	4.8	688.94	Good
	BH21	8.082	5.925	44	24	210	3.9	314.16	Excellent
Ibalebo-Adadama	BH22	8.099	5.929	36	29	21	2.3	31.28	Excellent
	BH23	8.115	5.934	47	29	445	1.7	664.24	Good
Ikpalegwa	BH24	8.117	5.935	38	29	295	3.4	439.76	Good
	BH25	8.117	5.936	36	34	101	2.4	150.06	Excellent
	BH26	8.145	5.937	97	27	13	1.8	19.20	Excellent
Igbo Imabana	BH27	8.158	5.940	89	26	624	3.1	931.00	Permissible
	BH28	8.160	5.944	75	36	191	3.8	285.48	Good
	BH29	8.045	5.992	45	26	591	4.7	882.00	Permissible
Ediba	SW1	8.022	5.851	29	25	200	3.9	298.00	Good
Afafanyi-Beach (Cross River)	SW2	7.990	5.887	18	28	35	3.2	52.64	Excellent
	SW3	8.013	5.875	17	28	33	4.1	48.88	Excellent
	SW4	8.022	5.878	19	28	33	4.4	49.82	Excellent
Ediba-Beach (Cross River)	SW5	8.022	5.879	16	28	33	4.6	48.88	Excellent
	SW6	8.023	5.880	18	28	33	4.6	49.82	Excellent
Itigidi-Beach (Cross River)	SW7	8.023	5.882	18	28	33	4.7	49.82	Excellent
Itigidi-Ekureku road	SW8	8.035	5.910	29	30	148	7.3	271.40	Good
Ekureku	SW9	8.017	5.993	47	27	125	2.5	286.24	Good
Lekokol-Atanl	SW10	8.091	5.928	34	28	68	5.2	101.52	Excellent
	SW11	8.091	5.928	33	23	90	4.8	334.16	Good
Ibalebo-Beach (Cross River)	SW12	8.102	5.930	18	29	34	4.2	50.60	Excellent
	SW1329 29	8.103	5.930	17	29	34	4.8	50.60	Excellent
Ekori-Beach (Cross River)	SW14	8.103	5.929	19	29	34	5.2	50.60	Excellent
	World Health Organization (2004)					500	7.5		

Table 1 continued

Location	Water sample type	Coordinates (°)		Elevation (m)	Temperature (°C)	TDS (mg/l)	pH	Measured conductivity corrected to 25 °C (µS/cm)	Water class for irrigation purposes*
		Longitude (E)	Latitude (N)						
Maximum					36	623.77	7.3	931.00	
Minimum					23	12.86	1.2	19.20	

BH borehole, *SW* surface

* According to Ragunath (1987)

Table 2 Results of soil sample analysis

S/no	Sample location	Coordinates (°)		EC (mS/cm)		pH
		Longitude (E)	Latitude (N)	Direct	VES	
1	Adadama cassava farm	8.098	5.941	6.0	4.83	5.22
2	Ekureku rice farm 1	8.039	5.945	10.0	12.66	5.13
3	Ekureku rice farm 2	8.021	5.994	10.0	12.66	4.53
4	CRS Agric. Dev. Project site	8.032	5.987	6.0	8.93	5.04
5	Usumutong-Ageugo cassava farm	8.003	5.877	7.0	4.60	4.93
6	Usumutong-Ebom cassava farm	8.002	5.837	5.0	2.89	4.75
7	Usumutong	8.013	5.847	6.0	3.52	4.70
8	Ediba-Usumutong	8.012	5.827	10.0	11.49	6.55
9	Agbara	8.012	5.996	14.0	14.08	4.60
10	Ediba	8.029	5.863	7.0	11.49	4.88
	Maximum	–	–	14.0	14.08	6.55
	Minimum	–	–	5.0	2.89	4.53
	Average	–	–	8.1	8.72	5.03

the VES and ERT data sets. The converted electrical resistivity data were manually plotted and where necessary, standard curve smoothening procedures were applied to the data (Bhattacharya and Patra 1968). Preliminary interpretation of the smoothened curves was done using partial curve matching technique (Orellana and Mooney 1966) to obtain initial layer parameters (depths and resistivities). Inversion of the original VES data was performed using a computer program called RESIST. The RESIST program performed automated approximation of the preliminary layer parameters generated from the manual curve matching phase (Vender Velpen 1988) while borehole lithologic data was used to constrain the results in order to reduce interpretational ambiguities. The root mean square (RMS) error technique in which 5 % was fixed as the upper acceptable limit was used in quantifying the difference between the theoretically generated and the measured VES data.

Results observed from the computer modelling process represent improved versions of the manually interpreted results. The borehole lithologic information collected from

the Rural Water Supply and Sanitation Agency (RU-WATSSA), Calabar, was placed side by side with closest VES models. A good correlation was observed between the electrical resistivity derived 1-D models and the borehole lithologs. Examples of some modelled VES curves and their correlation with closest borehole logs are shown in Fig. 2. The Kriging gridding method available in SURFER 11 computer program from Golden Software Inc., USA was used in contouring some of the observed parameters including soil salinity distribution at AB = 10 m and AB = 60 m (Fig. 3) and electrical resistivity values observed at AB = 4, 10, 20, 40, 60 and 100 m. The contoured resistivity sections observed for the different ABs slices were stacked to form the 3-D representation shown in Fig. 4.

The ERT data were analysed using the RES2DINV software (Loke and Barker 1996; Loke et al. 2003) that used the finite difference modelling subroutine and a non-linear smoothness-constrained least-squares optimization method to calculate the apparent resistivity and the resistivity values of the model blocks, respectively (De
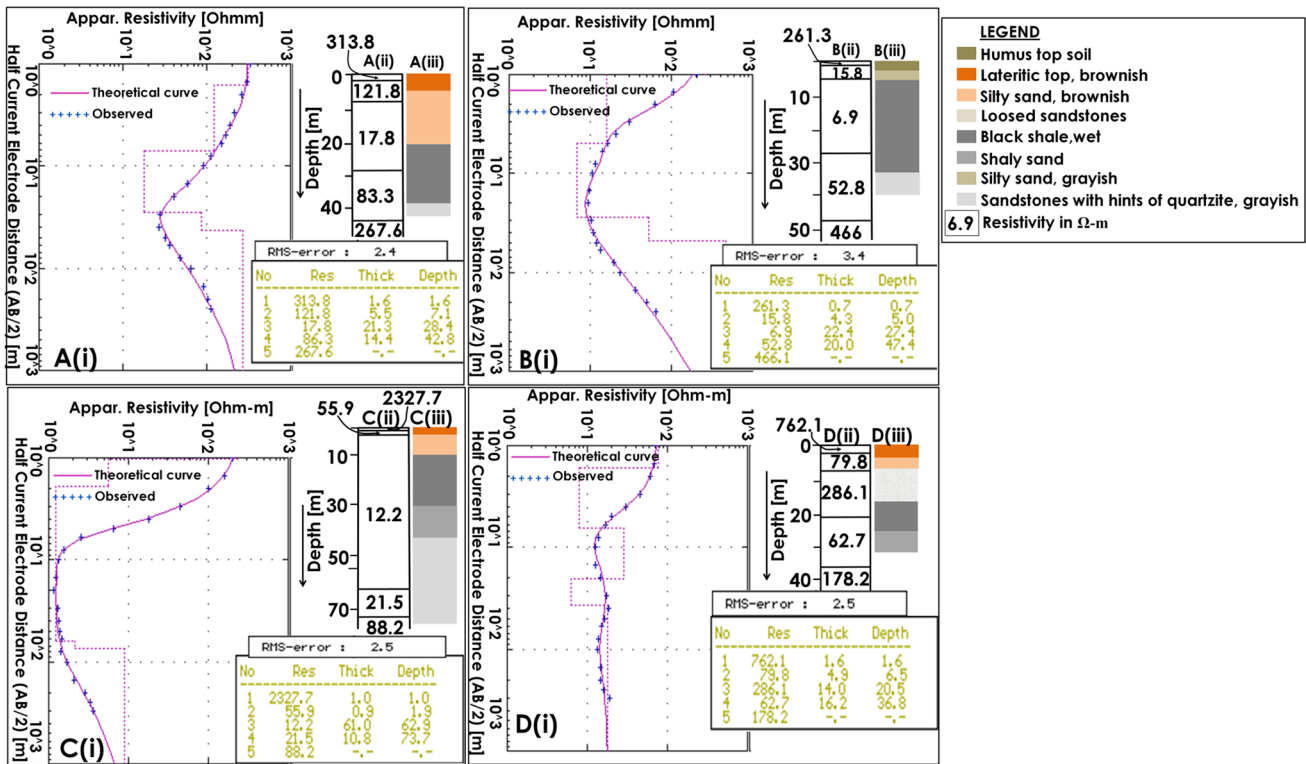
Fig. 2 Samples of modelled VES curves observed at **a** Egboronyi, **b** Adadama 1, **c** Agbara and **d** Ilike Communities. *Insert* Correlation of borehole lithologs with inverted VES results
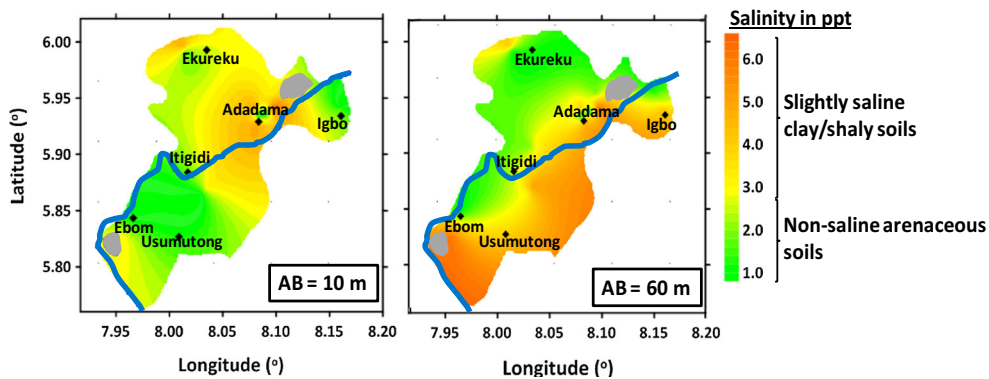

Fig. 3 Observed salinity distribution in parts per thousand (ppt) from resistivity data at AB = 10 m (**a**) and AB = 60 m (**b**)

Groot-Hedlin and Constable 1990). The RES2DINV software transformed the measured ERT data to an approximate picture of the true subsurface resistivity distribution and geometry of the subsurface features (Olayinka and Yaramanci 2000). This procedure produces smooth variations in subsurface resistivity distribution with depth (Loke et al. 2003) especially when constrained with geologic data. The algorithm subdivides the subsurface into rectangular grids equal in number to the number of data points and iteratively adjusts the resistivity model of each block by minimising the difference between the observed and the calculated resistivity values. The difference between these two sets of data was quantified using the RMS error technique in which 10 % was set as the upper acceptable threshold value. Representative samples of the ERT generated images are shown in Figs. 5, 6 and 7.

The modelled resistivity (ρ) values were transformed to SEC domain (mS/cm) using the relationship EC $= \sigma = \frac{1}{\rho}$. Then the observed SEC were corrected to 25 °C datum temperature required in the specific conductivity (SC_{25}) relationship (Myerchin et al. 2007) as:
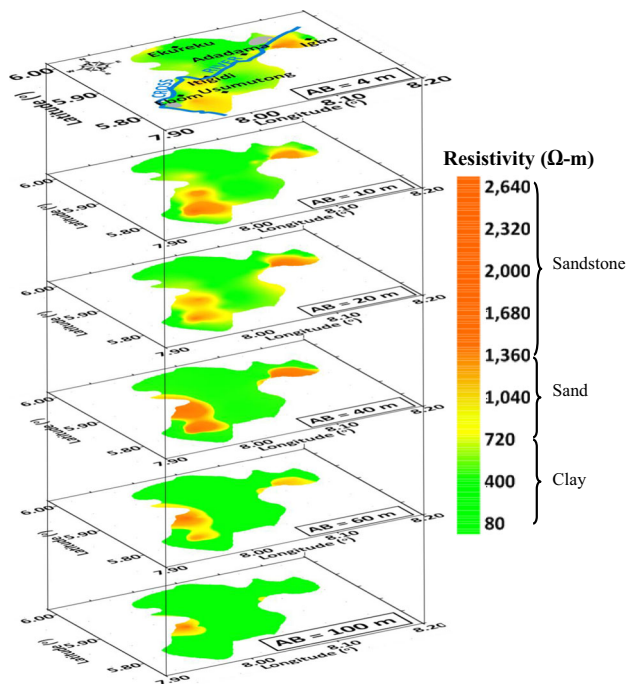
Fig. 4 Stacked contour maps showing lateral and vertical resistivity distribution in ohm–m of rocks and soils in the entire area

$$SC_{25} = \frac{EC_o(T)}{1 + r(T - 25)} \tag{4}$$

where $EC_o(T)$ is the observed bulk SEC at temperature T (°C) and r is the temperature correction coefficient of 2/°C. The temperature correction coefficient used in correcting the bulk SEC to the 25 °C datum was arrived at from the observation that every 1 °C rise in temperature usually result in 2 % increase in SEC (Grisso et al. 2009). Soil salinity was estimated from the SC_{25} values using the Weyl (1964) conversion table that relates soil conductivity at different temperatures with salinity (Table 3).

A graphical approach that Sikandar et al. (2010) adopted in interpreting the relationship between the measured WEC and VES generated bulk aquifer resistivity was also used to decipher the relationship between WEC and ρ. Although 55 VES points were acquired out of which 10 were repetitions, only 13 VES points that had boreholes and hand pumped wells in their neighbourhood were eventually selected for the graphical analysis. From the graphical analysis (Fig. 8), the WEC is related to ρ as:
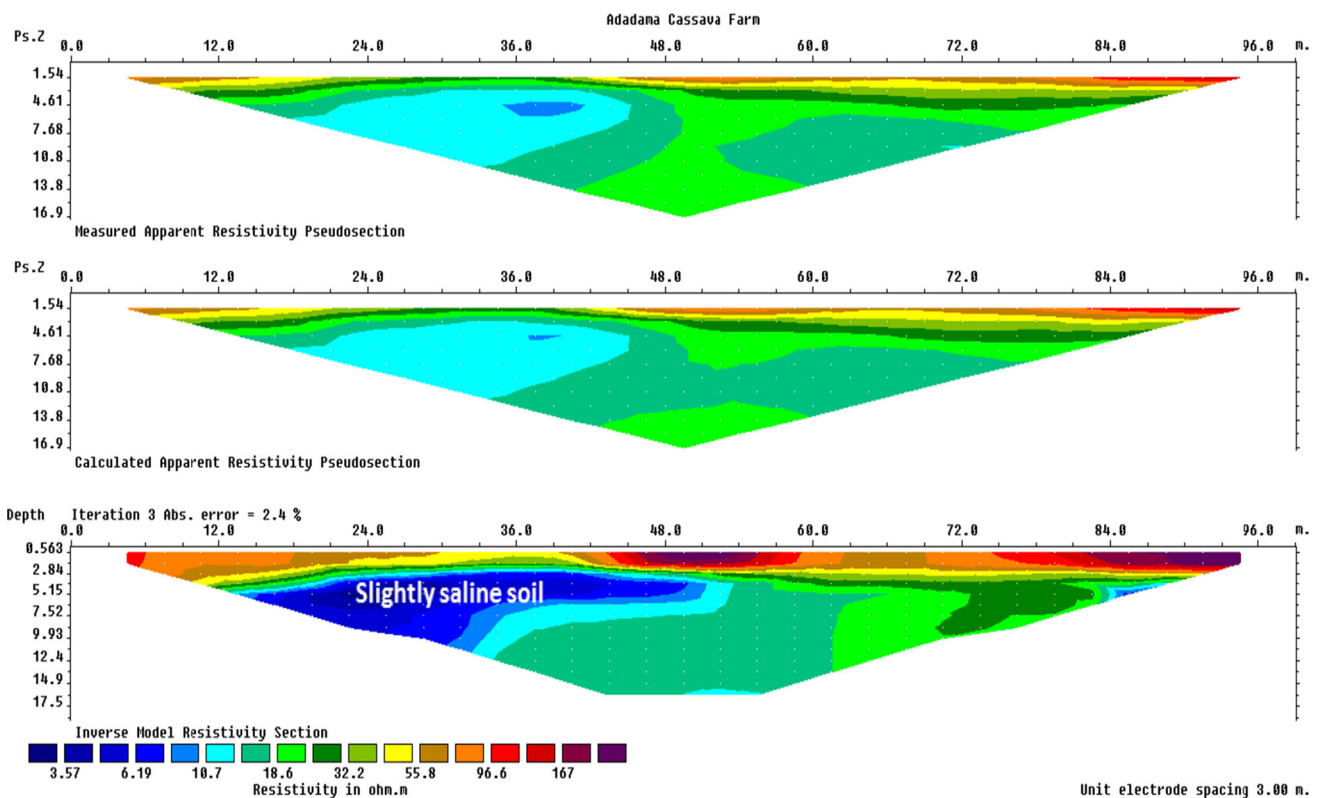
$$WEC = 65.007\rho^{-1.031} \tag{5}$$
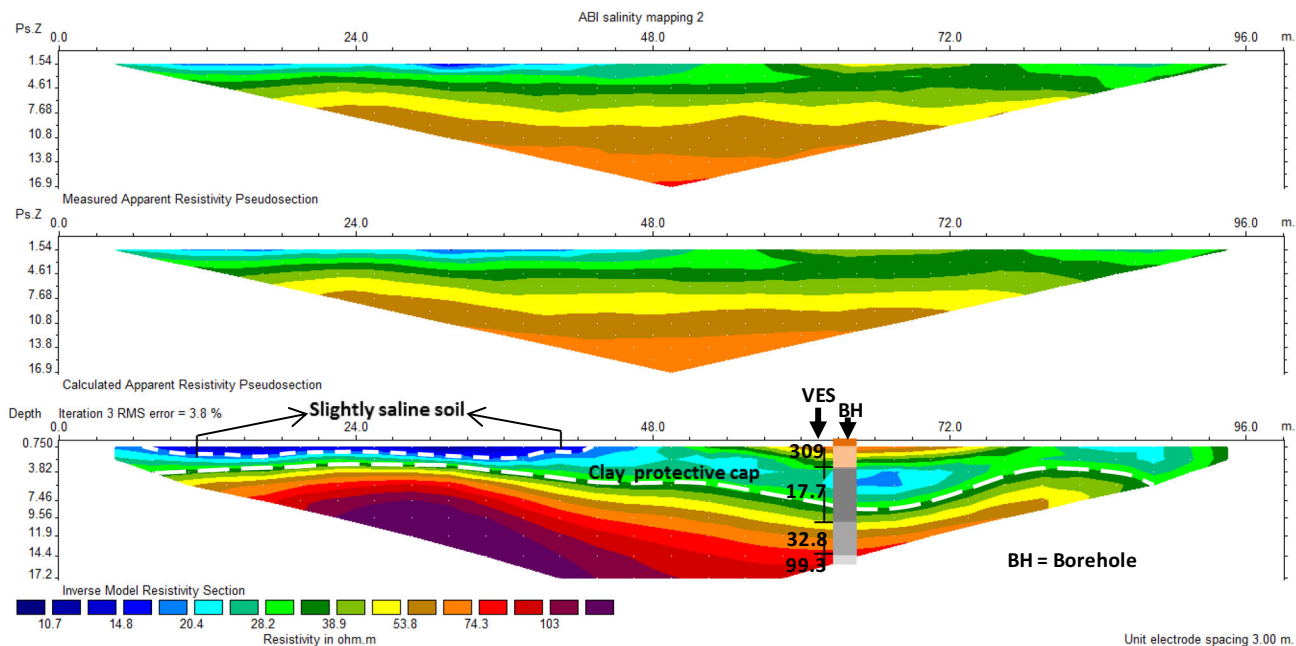

Fig. 5 ERT profile for Adadama Cassava Farm

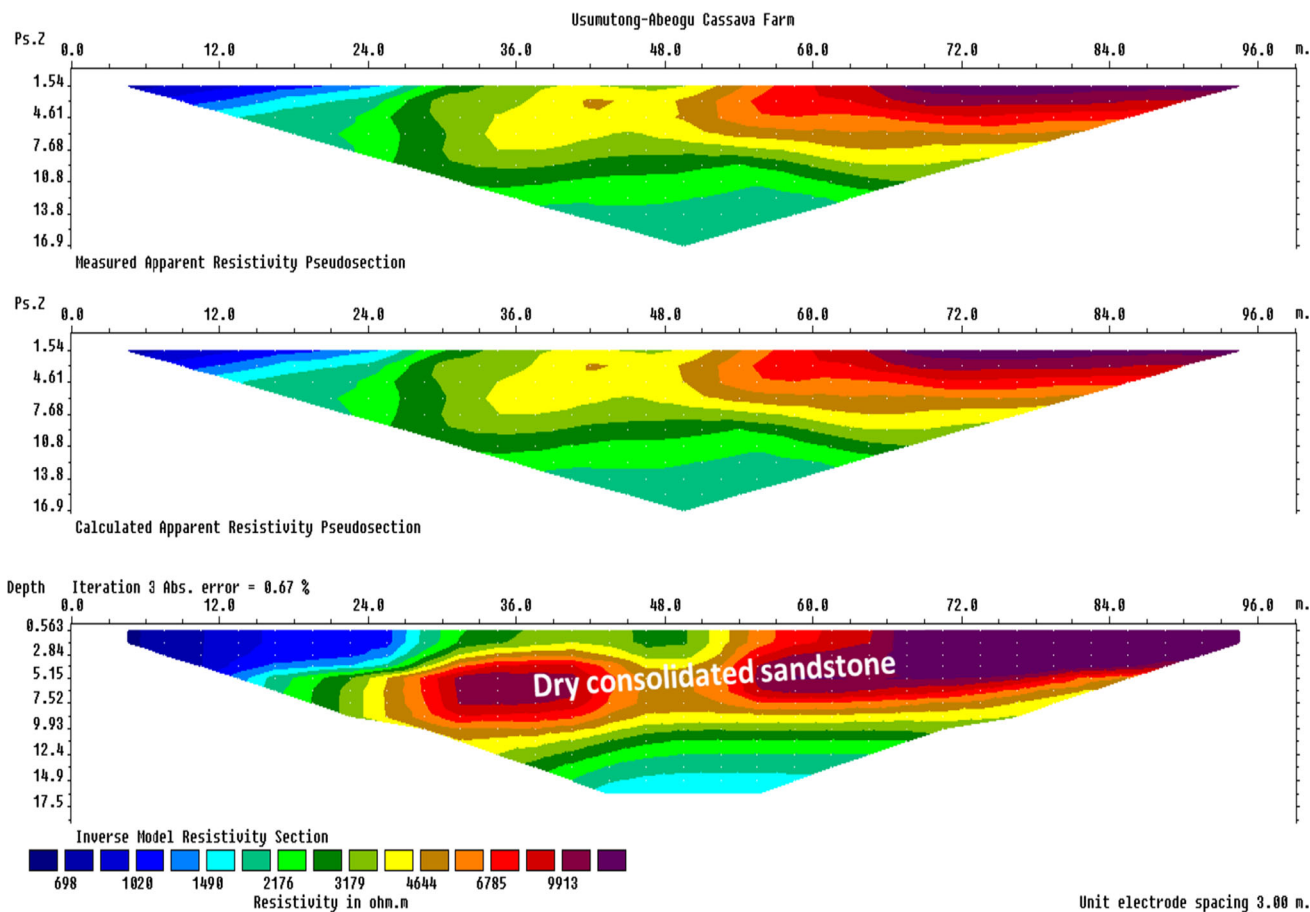**Fig. 6** ERT profile for Ekureku Rice Farm

Fig. 7 ERT profile for Usumutong-Abeogu Cassava Farm

Table 3 VES derived soil salinity at various depths

Location	VES no.	Coordinates (°)		AB/2 (m)	ρ_a (Ωm)	σ (mS/cm)	Weyl (1964) salinity rating (ppt)	Estimated depth range (m)
		Longitude	Latitude					
Adadama 1	1	8.0975	5.9407	2	62.05	1.61		0.00–0.67
				5	16.21	6.17	3	0.67–1.67
				10	10.66	9.39	5	1.67–3.33
				20	9.50	10.52	6	3.33–6.67
				30	10.16	9.85	6	6.67–10.0
				50	11.99	8.34	5	10.0–16.67
Ngoli	4	8.0848	5.9312	2	100.77	0.99		0.00–0.67
				5	35.83	2.79	1	0.67–1.67
				10	18.18	5.50	3	1.67–3.33
				20	18.03	5.55	3	3.33–6.67
				30	10.16	9.85	6	6.67–10.0
				50	7.87	12.71	7	10.0–16.67
Itabongho	8	8.0828	5.9286	2	707.24	0.14		0.00–0.67
				5	41.83	2.39	1	0.67–1.67
				10	13.94	7.17	4	1.67–3.33
				20	12.15	8.23	4	3.33–6.67
				30	14.46	6.92	4	6.67–10.0
				50	24.92	4.01	2	10–16.67
Agbara	11	8.0124	5.9963	2	1,005.88	0.10		0.00–0.67
				5	65.22	1.53		0.67–1.67
				10	13.26	7.54	4	1.67–3.33
				20	11.49	8.70	5	3.33–6.67
				30	14.12	7.08	4	6.67–10.0
				50	14.54	6.88	5	10–16.67
Anong Ezege	19	8.0356	5.8697	2	371.81	0.27		0.00–0.67
				5	68.97	1.45		0.67–1.67
				10	15.60	6.41	3	1.67–3.33
				20	10.72	9.33	5	3.33–6.67
				30	12.10	8.26	5	6.67–10.0
				50	15.62	6.40	4	10–16.67
Ilike	27	8.1598	5.9400	2	96.89	1.03		0.00–0.67
				5	83.64	1.20		0.67–1.67
				10	38.80	2.58	2	1.67–3.33
				20	18.96	5.28	3	3.33–6.67
				30	14.98	6.67	4	6.67–10.0
				50	15.98	6.26	4	10–16.67
Mboti	28	8.1603	5.9429	2	122.88	0.81		0.00–0.67
				5	79.41	1.26		0.67–1.67
				10	56.59	1.77	1	1.67–3.33
				20	27.32	3.66	2	3.33–6.67
				30	22.40	4.46	3	6.67–10.0
				50	20.91	4.78	3	10.0–16.67

Table 3 continued

Location	VES no.	Coordinates (°)		AB/2 (m)	ρ_a (Ωm)	σ (mS/cm)	Weyl (1964) salinity rating (ppt)	Estimated depth range (m)
		Longitude	Latitude					
Police ST. Adadama	36	8.0810	5.9405	2	148.58	0.67		0.00–0.67
				5	34.92	2.86	1	0.67–1.67
				10	12.99	7.70	4	1.67–3.33
				20	16.69	5.99	3	3.33–6.67
				30	14.48	6.91	4	6.67–10.0
				50	14.18	7.05	4	10.0–16.67
	37	8.0958	5.9539	2	134.11	0.75		0.00–0.67
				5	53.28	1.88		0.67–1.67
				10	19.27	5.19	3	1.67–3.33
				20	23.16	4.32	3	3.33–6.67
				30	29.73	3.36	2	6.67–10.0
				50	27.93	3.58	2	10.0–16.67
Ijum Lake	39	7.9568	5.8260	2	340.17	0.29		0.00–0.67
				5	97.99	1.02		0.67–1.67
				10	23.36	4.28	3	1.67–3.33
				20	10.28	9.73	6	3.33–6.67
				30	9.22	10.84	6	6.67–10.0
				50	9.61	10.41	6	10.0–16.67
Minimum					7.87	0.10	1	
Maximum					1,005.88	12.71	7	
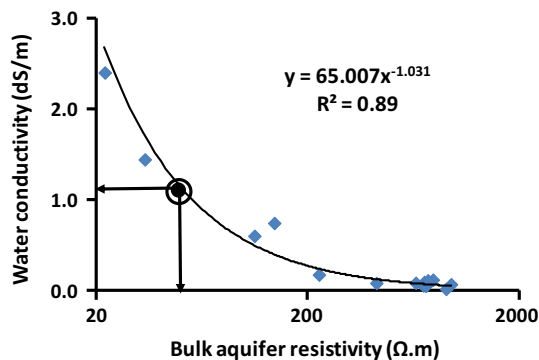
Fig. 8 Graph of bulk aquifer resistivity against water conductivity

with a correlation coefficient (R^2) of 0.89 which indicates a strong relationship between the two parameters.

Discussion of results

Resistivity and soil salinity distribution

The stacked contour resistivity slices (Fig. 4) capture both the lateral and vertical resistivity variations. Close to the surface, resistivity tends to vary significantly on both sides of the Cross River, which seems to divide the entire area into two halves (Fig. 4). Figure 4 shows that the area is dominated by two major resistivity domains. The first group has bulk resistivity above 100 Ωm and is more prevalent in the southwestern and northeastern areas where arenaceous materials abound. The spatial locations of these high resistivity materials correspond to the position of the sandstone ridges. At depths of ∼50 m in some locations, these high resistivities correspond to the electrical signatures of saturated lenticular sands. Electrical signatures of these arenaceous materials are conspicuous even at AB = 150 m. Materials with moderately high resistivity values dominate the second group. Bulk resistivity values of these materials are less than 100 Ωm and the low-lying argillaceous materials, which are prevalent in the northern parts of the study area, are prominent members of this group. Moderately high resistivities observed near the surface, decreased with depth to less than 50 Ωm especially in the northeastern, northwestern, southeastern and southern portions of the area. These sediments are prominent at AB = 20, 40, 60 and 100 m resistivity slices (Fig. 4) although sandstone materials occasionally truncate their lateral continuity. In the wet season, the bulk resistivities of the shaly materials at AB = 4 m were observed to be lower than its dry season counterparts possibly due to dissolved salty materials deposited there by surface runoff (Egboka and Okpoko 1984). These materials have

Table 4 Salinity levels in soils and their electrical conductivity at temperature $t = 25\ °C$

Salinity levels in soils	EC (mS/cm) at $t = 25\ °C$
Non-saline	0–2
Low salinity	2–4
Mild salinity	4–8
High salinity	8–16
Severe salinity	>16

resistivities (<100 Ωm) (Table 3) and were inferred to have low to high salinity according to the general soil salinity classification shown in Table 4 and correlates well with results of the direct measurement. The decrease in resistivity with depth could be as a result of exchange of ions, which tends to separate the clay minerals and consequently, allow them go into solution thus increasing their ionic concentration. In Fig. 3a, b, variation in salinity seems to trend in a predominant NE–SW direction, which corresponds to the dominant trend of geologic structures in the area. This supports the assertion that salinization in the area is controlled partly by geologic structures (Tijani et al. 1996; Tijani 2004). Although most of the soils and sediments (>10 m) are slightly saline, salinity levels are generally higher (≥3mS/cm) in the eastern and southern parts where argillaceous materials dominate. In the northwestern parts of the study area, salinity levels were slightly <3 mS/cm possible due to the dominance of silty sand materials.

The major shallow lithostratigraphic units in the area and their soil covers are captured in the ERT derived images of Figs. 5, 6 and 7. The shallow subsurface image of Adadama area (Fig. 5) obtained in a Cassava farm, shows that the upper layer is a thin (<4 m) sand dominant humus soil with bulk resistivity values that vary between 50 and 200 Ωm. These sandy materials dominate the entire ERT profile up to ∼4 m depth and lie almost parallel to the underlying materials. Under the sand-dominated upper layer is an electrically heterogeneous material with characteristic bulk resistivities <40 Ωm. These low resistivities were attributed to the prevalence of clayey/shaly materials near the surface. The presence of electrical heterogeneities at shallow depth was attributed to variations in moisture content and textural characteristics of these materials (Chambers et al. 2011). These clayey/shaly materials are thicker than the overlying materials and dominate the entire ERT profile from ∼4 m and extend beyond 15 m depth. The clay contents are more in the first 50 m along the profile where bulk resistivities <10 Ωm are predominant. The relatively high resistivity values observed in some portions of the profile are likely evidence of locally induced compaction that have resulted from agricultural and other human activities in the area.

The subsurface image generated from a rice farm in Ekureku area (Fig. 6) shows that the upper layer is dominated by low resistivity ($\rho < 40$ Ωm) argillaceous materials. About 50 m along the profile, the clay materials dip gently and reach depths of ∼10 m with a thin sandy clay material ($\rho \leq 60$ Ωm) overlying it between 55 and 75 m along the profile. Sediments with a predominantly sandy character (ρ is between 40 and 120 Ωm) underlie the clayey/shaly materials from ∼4 m depth at beginning of the profile to about 10 m towards the end of the profile. These sandy materials extend beyond 18 m below the surface and are locally saturated.

The ERT image of Usumutong area (Fig. 7) was generated at a clay-sandstone interface with the subsurface materials displaying high resistivity signatures ($\rho > 500$ Ωm) everywhere. From the beginning of the profile up to ∼30 m, gravelly clays and claystones materials with resistivity values <800 Ωm are dominant. These claystone materials extend to depths of ∼5 m below the surface and are underlain by materials with comparatively higher resistivity >800 Ωm, reflective of a sandstone-dominated lithology. Surficial exposures of these materials along the profile were used as the basis for these interpretations. Towards the end of the profile, the sandstone materials display a predominantly homogeneous character. The sandstone materials dip gently downward towards the beginning of the profile. The spatial location of the high resistivity zones correlate well with locations where surface exposures of Amaseri Sandstones in Afikpo Basin exist. Underlying the sandstone materials is a laterally homogeneous layer with moderate resistivity values (<800 Ωm).

The ERT derived subsurface images compare favourably well with their VES derived counterpart (Fig. 6). The high resistivity sand and low resistivity clay intercalations observed in the ERT images are in good agreement with the VES derived resistivity distribution. The depth to groundwater in the area can be grouped into very shallow (<30 m) and moderately shallow (30–70 m). Evapotranspiration is likely to exert significant influence on groundwater salinity conditions of the shallow groundwater. According to Bouwer (1978) and Stephens (1996), whenever the groundwater table is less than 9 m, soil gas humidity will be low thus increasing the rate of water loss by evapotranspiration. Salinity contributions from other soil salinity enriching factors such as the less abundant phreatophytic and lithic materials will be negligibly small since their salinity levels are far below harmful limits.

The groundwater samples have different WECs, TDS, temperature and pH values and therefore seem to have originated from different aquifers. These observations are in accordance with the findings of Akpan et al. (2013), who observed that the groundwater flow in the area are localised

due to blocking of the water flow paths by the sandstone ridges and other structural discontinuities. Using the irrigation water classification scheme (Ragunath 1987), 5 % of the water in the area currently falls under the permissible class, 42 % falls under the good class while the remaining 53 % falls under the excellent class (Table 1). These results conform with the findings of Akpan et al. (2013) who observed that the water resources in the IME belong to the good–excellent class for irrigation purposes. Using a cutoff resistivity of 50 Ωm (Fig. 8), the groundwater in the area fits into two dominant classes for irrigation purposes (Sikandar et al. 2010). Thus, groundwater with resistivity >50 Ωm are fit for irrigation purposes while those with resistivity <50 Ωm are marginally fit for irrigation purposes (Sikandar et al. 2010). Generally, WEC of samples were classified to be fresh and slightly saline according to Hamzah et al. (2007) water classification scheme (Table 5). WEC <700 μS/cm are fresh and those within the range 700–2,000 μS/cm are classified to be slightly saline. The WEC in the area is generally <750 μS/cm except in Igbo Imabana area where conductivity values >750 μS/cm were observed. This observation shows that the water resources (surface and ground) in the low WEC areas are fresh and belong to the good–excellent class while in the high WEC areas, the water is slightly saline or brackish and belong to the permissible class (Richards 1954). The TDS and pH values of the water were observed to be <650 mg/L and ≤7.3, respectively.

In all the sites investigated, the shallow subsurface materials under the rice farms were characterised by low resistivities ($\rho < 50$ Ωm) that overlie comparatively high resistivity sandy materials ($\rho > 50$ Ωm) at deeper depths. The interface between the sandy and the clayey materials appears to be occupied by materials of anthropic origin. As pointed out by Levi et al. (2008), from results of the direct salinity measurement coupled with our knowledge of the general hydrogeology of the area, locations with bulk resistivity <50 Ωm are slightly saline zones while locations with higher resistivity values are fresh water zones. Thus, based on the resistivity values, the shallow subsurface in

the low-lying areas are generally stratified into slightly saline (the low resistivity zones) and fresh water (the high resistivity) environments. As stated earlier, the interface between the low and high resistivity materials is occupied by materials that are basically of anthropogenic origin. Where observed, the moderate resistivity sandy materials are good aquifers and the groundwater is protected from contamination by the overlying clay materials although their effectiveness might be limited by their vertical extent.

From the results of the soil analyses (Table 2), values of the soil salinity were observed to vary between 5.0 mS/cm at a Cassava farm in Usumutong to 14.0 mS/cm at a rice farm in Agbara Community. These results corroborate well with minimum and maximum variations of 2.89 at the same Usumutong and 14.08 mS/cm at Agbara areas estimated using the VES technique, respectively. The estimated bulk soil salinity increases with depth from ∼1–3 part per thousand (ppt) at depths of ∼0.7–3.3 m in the north and northwestern areas and increases with depth to ∼4–6 ppt within the depth range of ∼3.3–16.7 m (Table 3). Maximum and minimum variations in soil pH were observed to be 4.53–6.55, respectively, thus capturing the soils as being a slightly acidic medium. The salinity state of the soils is not beyond safe limits and so will not disturb the normal growth of some plants (Rhoades et al. 1999; Udo et al. 2009).

The observed variations in salinity in the area seem to have originated from both natural and anthropogenic sources. As discussed above, shallow depth to groundwater table enhances evapotranspiration rates (Egboka and Okpoko 1984; Okoyeh et al. 2013). High rates of evapotranspiration leave the superficial water in a more saline state (Hibbs 2001; Papaioannou et al. 2007). Topographic and hydraulic induced forces will cause saline-enriched water to flow, once the threshold conditions (Lobkovsky et al. 2004) necessary for such flows are exceeded. The subsurface flowing groundwater usually emerges as ephemeral seepages, springs, streams and ponds along road-cuts and hills at very low flow rates in the wet season. These seepages normally flow downward and will accumulate in the poorly drained and swampy low-lying areas. Accumulation of such slightly saline water will eventually raise the existing salinity levels of the water and soils.

The poorly drained and swampy areas are zones where the local farmers commonly practice active cultivation of paddy rice and other cereal crops (e.g., maize). The local farmers have been applying yield enhancement inorganic chemicals such as fertilizers and other chemical composites, pesticides and herbicides and where necessary, irrigation practices in these areas for a long time. Of all the productivity enhancement practices, application of inorganic fertilizers, which are enriched with leachable

Table 5 Water class and electrical resistivity

Water class	Electrical resistivity (Ω–m)	
	Measured	Hamzah et al. (2007)
Fresh	22–647	700
Slightly saline	703–780	700–2,000
Moderately saline	–	2,000–10,000
Highly saline	–	10,000–25,000
Very highly saline	–	25,000–45,000
Brine (seawater)	–	>45,000

substances like nitrates (NO_3^-) is more rampant. Severe leaching and transportation of the dissolved chemical components of the inorganic fertilizers beyond the root zone of most crops by percolating irrigation water and continuous torrential rainfall that characterise the area are likely contributors to the marginal increase in soil salinity (Singh et al. 2011; Akpan et al. 2013). According to Barros et al. (2012) and Wood et al. (2000), flat and poorly drained agricultural lands are characterised by elevated salinities. The implication of the elevated salinity in the low-lying areas is that the growth and yield of some plants may be impaired thereby threatening the sustainability of food production. Extreme cases of such increased salinity could also adversely affect soils and human health (Udo et al. 2009; Barros et al. 2012). However, the salt concentration in the soils are good enough to support the growth of some salt-tolerant crops.

Conclusion

Joint analyses and interpretation of data generated from VES, 2-D ERT, soil and water samples from Abi area, Nigeria have shown that the soils, shallow sediments and water can be classified into non-saline, low salinity, mild salinity and high salinity soils/sediments and fresh to brackish or slightly saline water. The poorly drained soils where groundwater levels are less than 10 m below the surface were observed to be slightly saline and the salinity was observed to increase with depth in the northern and northwest portions. Human activities like uncontrolled application of inorganic fertilizer and high rate of evapotranspiration at the shallow groundwater areas were inferred to be the primary sources of salinity. However, concentrations of NO_3^- are likely to be low in swamp areas due to denitrification. Groundwater salinity is lower in locations where low resistivity argillaceous materials dominate the vadose zone. In locations where the aquifer systems are unconfined with permeable sand and silt layers, salinity levels are slightly higher.

Salinity mapping based on resistivity data provides good results needed for soil and groundwater assessment, protection, management and conservation. It can also be used as a tool for raising awareness about soil and groundwater risk when monitored for a certain period and can be recommended for large-scale investigation in precision agricultural practice and SEC mapping.

References

Acworth RI, Jorstad LB (2006) Integration of multi-channel piezometry and electrical tomography to better define chemical heterogeneity in a landfill leachate plume within a sand aquifer. J Contam Hydrol 83:200–220. doi:10.1016/j.jconhyd.2005.11.007

Adepelumi AA, Ako BD, Ajayi TR, Afolabi O, Omotoso EJ (2008) Delineation of saltwater intrusion into the freshwater aquifer of Lekki Peninsula, Lagos, Nigeria. J Environ Geol 56(5):927–933

Akpan AE, George NJ, George AM (2009) Geophysical investigation of some prominent gully erosion sites in Calabar, southeastern Nigeria and its implications to hazard prevention. Disaster Adv 2(3):46–50

Akpan AE, Ugbaja AN, George NJ (2013) Integrated geophysical, geochemical and hydrogeological investigation of shallow groundwater resources in parts of the Ikom-Mamfe Embayment and the adjoining areas in Cross River State, Nigeria. J Environ Earth Sci 70(3):1435–1456. doi:10.1007/s12665-013-2232-3

Arango-Galván C, De la Torre-González B, Chávez-Segura RE, Tejero-Andrade A, Cifuentes-Nava G, Hernández-Quintero E (2011) Structural pattern of subsidence in an urban area of the southeastern Mexico Basin inferred from electrical resistivity tomography. Geofís Int 50(4):401–409

Archie GE (1942) The electrical resistivity logs as an aid in determining some reservoir characteristics. Trans Am Inst Min Metall Eng J 146:54–62

Barros R, Isidoro D, Aragüés R (2012) Three study decades on irrigation performance and salt concentrations and loads in the irrigation return flows of La Violada irrigation district (Spain). Agric Ecosyst Environ 151:44–52

Benkabbour B, Toto EA, Fakir Y (2004) Using DC resistivity method to characterize the geometry and the salinity of the Plioquaternary consolidated coastal aquifer of the Mamora plain, Morocco. J Environ Geol 45:518–526. doi:10.1007/s00254-003-0906-y

Benkhelil J (1982) Benue Trough and Benue Chain. Geol Mag J 119:115–168

Beriss FE, Schjønning P, Keller T, Lamandé T, Etana A, de Jonge LW, Iversen BV, Arvidsson J, Forkman J (2012) Persistent effects of subsoil compaction on pore size distribution and gas. Soil Tillage Res 122:42–51. doi:10.1016/j.still.2012.02.005

Bhattacharya BB, Patra HP (1968) Direct current in geoelectric sounding, methods in geochemistry and geophysics 9. Elsevier, Amsterdam, p 136

Bouwer H (1978) Groundwater Hydrology. McGraw-Hill Book Co, New York, p 480

Bussain AE (1983) Electrical conductance in a porous medium. Geophysics 48(9):1258–1268

Cardarelli E, Cercato M, Cerreto A, Di Filippo G (2010) Electrical resistivity and seismic refraction tomography to detect buried cavities. Geophys Prospect J 58:685–695

Chambers JE, Wilkinson PB, Kuras O, Ford JR, Gunn DA, Meldrum PI, Pennington CVL, Weller AL, Hobbs PRN, Ogilvy RD (2011) Three-dimensional geophysical anatomy of an active landslide in Lias Group mudrocks, Cleveland basin, UK. Geomorphology 125(4):472–484. doi:10.1016/j.geomorph.2010.09.017

Chang SW, Clement TP, Simpson MJ, Lee KK (2011) Does sea-level rise have an impact on saltwater intrusion? Adv Water Resour 34:1283–1291. doi:10.1016/j.advwatres.2011.06.006

De Groot-Hedlin C, Constable S (1990) Occam's inversion to generate smooth, two dimensional models from magnetotelluric data. Geophysics 55:1613–1624

Ebong ED, Akpan AE, Onwuegbuche AA (2014) Estimation of geohydraulic parameters from fractured shale and sandstone aquifers of Abi (Nigeria) using electrical resistivity and

hydrogeologic measurements. J Afr Earth Sc 96C:99–109. doi:10.1016/j.jafrearsci.201403.026

Edet A, Nganje TN, Ukpong AJ, Ekwere AS (2011) Groundwater chemistry and quality of Nigeria: A status review. Afr J Environ Sci Technol 5(13):1152–1169. doi:10.5897/AJESTX11.011

Egboka BCE, Okpoko EI (1984). Gully erosion in the Agulu-Nanka region of Anambra State, Nigeria. In: Changes in African hydrology and water resources (Proceedings of the Harare Symposium, July 1984). IAHS Publication no 144

Egboka BC, Uma KO (1986) Hydrogeochemistry, contaminant transport and tectonic effects in the Okposi-Uburu salt lake area of Imo state, Nigeria. Hydrol Sci J 31(2):205–221

Ekwueme BN, Nyong EE, Petters SW (1995) Geological excursion guide book to Oban Massif, Calabar Flank and Mamfe Embayment, Southeastern Nigeria, 1st edn. Dechord Press, Calabar, p 36

Eseme E, Agyingi CM, Foba-Tendo J (2002) Geochemistry and gneisses of brine emanations from cretaceous strata of the Mamfe Basin, Cameroon. J Afr Earth Sci 35(4):467–476

Gemail KS, El-Shishtawy AM, El-Alfy M, Ghoneim MF, Abd El-Bary MH (2011) Assessment of aquifer vulnerability to industrial waste water using resistivity measurements. A case study, along El-Gharbyia main drain, Nile Delta, Egypt. J Appl Geophys 75:140–150. doi:10.1016/j.jappgeo.2011.06.026

Gómez-Ortiz D, Martín-Velázquez S, Martín-Crespo T, Márquez A, Lillo J, López I, Carreño F, Martín-González F, Herrera R, De Pablo MA (2007) Joint application of ground penetrating radar and electrical resistivity imaging to investigate volcanic materials and structures in Tenerife (Canary Islands, Spain). J Appl Geophys 62:287–300. doi:10.1016/j.jappgeo.2007.01.002

Grisso R, Alley MM, Holshouser D, Thomason W (2009) Precision farming tools: soil electrical conductivity. Virginia Polytechnic Institute and State University, Virginia State

Hamzah U, Samsudin AR, Malim EP (2007) Groundwater investigation in Kuala Selangor using vertical electrical sounding (VES) surveys. Environ Geol 51(8):1349–1359

Hibbs BJ (2001) Geophysical and hydrochemical analysis of the White River alluvial aquifer. In: New Mexico Geological Society Guidebook, 52 nd Field Conference, Geology of the Llano Estacado. Crossby County, Texas, pp 309–316

Inoubli N, Gouasmia M, Gasmi M, Mharndi A, Ben Dhia H (2006) Integration of geological, hydrochemical and geophysical methods for prospecting thermal water resources: the case of the Hmeima region (central-western Tunisia). J Afr Earth Sc 46(3):180–186

Keller GV, Frischknecht FC (1966) Electrical methods in geophysical prospecting. Pergamon Press Inc, Oxford, p 519

Levi E, Goldman M, Hadad A, Gvirtzman H (2008) Spatial delineation of groundwater salinity using deep time domain electromagnetic geophysical measurements: A feasibility study. Water Res Res 44:W12404. doi:10.1029/2007WR006459

Lobkovsky AE, Jensen B, Kudrolli A, Rothman DH (2004) Threshold phenomena in erosion driven by subsurface flow. J Geophys Res 109:F04010. doi:10.1029/2004JF000172

Loke MH, Barker RD (1996) Rapid least-squares inversion of apparent resistivity pseudosections using a quasi-Newton method. Geophys Prospect 44:131–152

Loke MH, Acworth I, Dahlin T (2003) A comparison of smooth and blocky inversion methods in 2D electrical imaging surveys. Explor Geophys 34:182–187

Mao M, Chirwa EC, Chen T (2005) Vehicle roof crush modeling and validation. In: 5th European LS-DYNA users Conference. Birmingham

Metwaly M, Khalil M, Al-Sayed E, Osman S (2006) A hydrogeo-physical study to estimate water seepage from northwestern Lake Nasser, Egypt. J Geophys Eng 3:21–27

Michael HA, Mulligan AE, Harvey CF (2005) Seasonal oscillations in water exchange between aquifers and the coastal ocean. Nature 431:1145–1148

Minsley BJ, Ajo-Franklin J, Mukhopadhyay A, Morgan FD (2011) Hydrogeophysical methods for analyzing aquifer storage and recovery systems. Groundwater 49(2):250–269

Moore WS, de Oliveira J (2008) Determination of residence time and mixing processes of the Ubatuba, brazil, inner shelf waters using natural Ra isotopes. Estuar Coast Shelf Sci 76(3):512–521

Morreau C, Regnoult JM, Deruelle B, Robineau B (1987) A new tectonic model for the Cameroon Line, Central Africa. Tectonophysics 139:317–334

Myerchin GM, White DM, Lilly MR, Holland KM, Prokein P (2007) Lake survey data for the Kuparuk foothills region: Spring 2007. University of Alaska Fairbanks, Water and Environmental Research Center, Report INE/WERC 07.15. Fairbanks, Alaska

Nwankwoala HO (2011) Coastal aquifers of Nigeria: an overview of its management and sustainability considerations. J Appl Technol Environ Sanit 1(4):371–380

Odigi MI, Amajor LC (2008) Origin of carbonate cement in cretaceous sandstones from Lower Benue Trough, Nigeria: evidence from petrography and stable isotope composition. Sci Afr 7(2):123–139

Odigi MI, Amajor LC (2009) Geochemical characterization of cretaceous sandstones from the Southern Benue Trough, Nigeria. Chin J Geochem 28:044–054. doi:10.1007/s11631-009-0044-7

Ogilvy RD, Meldrum PI, Kuras O, Wilkinson PB, Chambers JE (2008) Advances in geoelectric imaging technologies for the measurement and monitoring of complex earth systems and processes. In: Proceedings 33rd International Geological Congress. Oslo, Norway

Okoyeh EI, Akpan AE, Egboka BCE, Okeke HI (2013) An assessment of the influences of surface and subsurface water level dynamics in the development of gullies in Anambra State, southeastern Nigeria. J Earth Interact 18:1–24

Olayinka AI, Yaramanci U (2000) Assessment of the reliability of 2D inversion of apparent resistivity data. Geophys Prospect 48(2):293–316. doi:10.1007/s10040-009-0503-6

Onwualu JN, Ukaegbu VU, Okengwu KO (2012) Source region inhomogeneity in igneous suite of Ishiagu, Southern Benue Trough, Nigeria. Arch Appl Sci Res 4(2):923–934

Orellana E, Mooney AM (1966) Master tables and curves for vertical electrical sounding over layered structures. Interciencia, Escuela, p 159

Papaioannou A, Plageras P, Dovriki E, Minas A, Krikelis V, Nastos PT, Kakavas K, Paliatsos AG (2007) Groundwater quality and location of productive activities in the region of Thessaly (Greece). Desalination 213:209–217. doi:10.1016/j.desal.0000.00.000

Poulsen SE, Rasmussen KR, Christensen NB, Christensen S (2010) Evaluating the salinity distribution of a shallow coastal aquifer by vertical multielectrode profiling (Denmark). Hydrogeol J 18(1):161–171. doi:10.1007/s10040-009-0503-6

Ragunath HM (1987) Ground water, 2nd edn. Wiley Eastern Ltd, New Delhi, p 563

Rhoades JD, Chanduvi F, Lesch S (1999) Soil salinity assessment: methods and interpretation of electrical conductivity measurements. Food and Agriculture Organization of the United Nations vol. 57. pp 165

Richards LA (1954) Diagnosis and improvement of saline and alkali soils. In: Agricultural Handbook 60. USDA and IBH Publishing Co. Ltd, New Delhi. pp 98–99

Samsudin AR, Haryono A, Hamzah U, Rafek AG (2007) Salinity mapping of coastal groundwater aquifers using hydrogeochemical and geophysical methods: a case study from north Kelantan,

Malaysia. Environ Geol 55(8):1737–1743. doi:10.1007/s00254-007-1124-9

Schutjens PMTM, Hanssen TH, Hettema MHH, Merour J, de Bree P, Coremans JWA, Helliesen G (2004) Compaction-induced porosity/permeability reduction in sandstone reservoirs: data and model for elasticity-dominated deformation. SPE Reserv Eval Eng 7(3):202–216. doi:10.2118/88441-PA

Sen PN, Goode PA, Sibbit A (1998) Electrical conduction in clay bearing sandstones at low and high salinities. J Appl Phys 63:4832–4840

Sikandar P, Bakhsh A, Arshad M, Rana T (2010) The use of vertical electrical sounding resistivity method for the location of low salinity groundwater for irrigation in Chaj and Rachna Doabs. J Environ Earth Sci 60:1113–1129. doi:10.1007/s12665-009-0255-6

Singh CK, Shashtri S, Mukherjee S (2011) Integrating multivariate statistical analysis with GIS for geochemical assessment of groundwater quality in Shiwaliks of Punjab, India. Environ Earth Sci 62(7):1387–1405

Stephens DB (1996) Vadose Zone Hydrology. Lewis Publishers, Boca Raton 347 p

Swarzenskis PW, Reich C, Kroeger KD, Baskaran M (2007) Ra and Rn isotopes as natural tracers of submarine groundwater discharge in Tampa Bay, Florida. Mar Chem 104:69–84. doi:10.1016/j.marchem.2006.08.001

Telford WM, Geldart LP, Sheriff RE (1990) Applied geophysics. Cambridge University Press, Cambridge 792 pp

Tijani MN (2004) Evolution of saline waters and brines in the Benue-Trough, Nigeria. J Appl Geochem 19:1355–1365. doi:10.1016/j.apgeochem.2004.01.020

Tijani MN (2008) Hydrochemical and stable isotopes compositions of saline groundwaters in the Benue Basin, Nigeria. In: Adelana S, MacDonald A (eds) Applied groundwater studies in Africa. IAH Selected papers on Hydrogeology vol. 13. pp 352–369

Tijani MN, Loehnert EP (2004) Exploitation and traditional processing techniques of brine salts in parts of the Benue Trough, Nigeria. Int J Miner Process 74:157–167

Tijani MN, Loehnert EP, Uma KO (1996) Origin of saline ground-waters in the Ogoja area, Lower Benue Basin. Nigeria. J Afr Earth Sci 23(2):237–252

Toushmalani R (2010) Application of geophysics in agriculture. Aust J Basic Appl Sci 4(12):6433–6439

Udo EJ, Ibia TO, Ogunwale JA, Ano AO, Esu IE (2009) Manual of soil, plant and water analyses. Sibon Books Limited, Festac, Lagos, p 183

Uma KO, Onuoha KM, Egboka BC (1990) Hydrochemical facies, groundwater flow pattern and origin of saline waters in parts of the western flank of the Cross River basin, Nigeria. In: Ofoegbu CO (ed) The Benue-Trough: structure and evolution. Vieweg Verlag, Braunschweig, pp 115–134

Vandenbohede A, Luyten K, Lebbe L (2008) Impacts of global change on heterogeneous coastal aquifers: a case study in Belgium. J Coast Res 24(2A):160–170

Vandenbohede A, Van Houtte E, Lebbe L (2009) Sustainable groundwater extraction in coastal areas: a Belgian example. Environ Geol 57:735–747

Vender Velpen BPA (1988) A computer processing package for DC resistivity interpretation for an IBM compatibles. ITC J 4

Wang DY, Song YC, Zhang Y, Liu Y, Zhao ML, Qi T, Zhao JF (2012) An approach for the numerical computation of the reduction of the original porosity due to diagenetic and compaction processes in sandstone reservoirs. J Adv Mat Res 383–390:6057–6060. doi:10.4028/www.scientific.net/AMR.383-390.6057

Weyl PK (1964) On the change in electrical conductance of seawater with temperature. Limnol Oceanogr 9:75–78

Wilkinson PB, Meldrum PI, Kuras O, Chambers JE, Holyoake SJ, Ogilvy RD (2010) High-resolution electrical resistivity tomography monitoring of a tracer test in a confined aquifer. J Appl Geophys 70:268–276. doi:10.1016/j.jappgeo.2009.08.001

Wood S, Sebastian K, Scherr SJ (2000) Soil resource condition. In: Wood S, Sebastian K, Scherr SJ (eds) Pilot analysis of global ecosystems. IFPRI and World Resources Institute, Washington

World Health Organization (2004) Guidelines for drinking water quality, vol 1, recommendations, 2nd edn. WHO, Geneva, p 130

YihdegoY Webb J (2012) Modelling of seasonal and long-term trends in lake salinity in southwestern Victoria, Australia. J Environ Manage 112:149–159

Young MB, Gonneea ME, Fong DA, Moore WS, Herrera-Silveira J, Paytan A (2007) Characterizing sources of groundwater to a tropical coastal lagoon in a karstic area using Radium isotopes and water chemistry. Mar Chem 109:377–394

Zarroca M, Bach J, Linares R, Pellicer XM (2011) Electrical methods (VES and ERT) for identifying, mapping and monitoring different saline domains in a coastal plain region (Alt Empordà, Northern Spain). J Hydrol 409:407–422. doi:10.1016/j.jhydrol.2011.08.052